05.1;09.6

Exploring principal stresses using holographic interferometry

© Yu.P. Borodin[1,2], V.V. Kesaev[1], A.N. Lobanov[1], S.A. Ambrozevich[1,3]

[1] Lebedev Physical Institute, Russian Academy of Sciences, Moscow, Russia
[2] MIREA - Russian Technological University, Moscow, Russia
[3] Bauman Moscow State Technical University, Moscow, Russia
E-mail: lobanovan@lebedev.ru

Received July 7, 2023
Revised August 7, 2023
Accepted August 29, 2023

A phenomenological model for the experimental determination of the principal stress magnitudes and directions using the holographic interferometry and probing hole method is proposed. This non-invasive *in situ* method allows for the analysis of stress-strain states for a wide range of objects. The model establishes a straightforward relationship between the interference order and planar stress magnitude. The presented results have a practical importance for assessing the performance capability and safety of technical objects, as well as of their components and parts, during commissioning or operation.

Keywords: holographic interferometry, probing hole method, planar stress state, non-destructive testing, measurement of principal stresses.

DOI: 10.61011/TPL.2023.10.57059.19678

One of the most important problems of mechanics and structural design is determination of mechanical stresses in the components of structures and mechanisms. Experimental methods for determining stresses in objects are of especial importance because they allow direct estimation of the stress state. Such methods that do not destroy the object and do not withdraw it from operation belong to the field of non-destructive examination whose goal is to reliably reveal dangerous defects or states. In practice, controlling the stress state is often a key operation whose cost is comparable with or even exceeds the cost of fabricating the test object itself. Indeed, destruction of critical components (boilers, mechanisms, welds, flanged joints, etc.) leads to catastrophic consequences. Therefore, methods for the stress state analysis and, especially, for its experimental determination, need continuous improvement.

This paper considers the method for experimental determination of stresses by drilling probing holes and also by the method of holographic interferometry proposed by domestic researchers in early 1980s [1,2]. Drilling the holes induces local axially-symmetric violation of the material continuity, which causes stress redistribution near the hole and, hence, deformations. For the interferometric method, relatively small probing hole diameter and depth (1−3 mm) are sufficient. Typically, such holes do not affect further serviceability of the test object and can be easily eliminated after the completion of measurements; therefore, this method may be regarded as non-invasive. The method, its experimental procedure and equipment, field of application and restrictions are described in more details in monography [3]. Notice that the relationship between the surface displacements and stresses causing them still remains a subject of research [4,5]. In the method under consideration, stresses are typically being determined by recalculating the results obtained for reference materials [3]. The goal of this study was to directly determine the numerical relationship between normal strain component u_z and absolute stress magnitudes $\sigma_{1,2}$, and also to establish directions α of principal planes in the laboratory frame of reference.

The procedure for experimental measurement of stresses consists of three successive steps. At the first step, the wavefront scattered from the surface free of hole is being recorded holographically. In our study, this was performed by using a non-disposable photo-thermoplastic material based on poly-N-vinylcarbazole which allows observing the reconstructed image in transmitted rays with a digital camera. The conditions for recording the hologram are shown in Fig. 1, *a*. They make the experiment sensitive to only normal displacements. For instance, in the case of the laboratory frame of reference with the X and Y axes directed arbitrary in the tangential plane, axis Z will be directed along normal $\hat{\mathbf{n}}$. Therefore, it is necessary to illuminate the object by a collimated light beam with a planar wavefront and wave vector $\hat{\mathbf{k}}_1$ directed along the normal ($\hat{\mathbf{k}}_1 \parallel \hat{\mathbf{n}}$). Then, the aperture of the recorded hologram should also allow observing the reconstructed wavefront along the normal. The diffusively reflecting surface of the object scatters light in all the directions; therefore, it is necessary to separate out a part of the reconstructed wavefront whose vector $\hat{\mathbf{k}}_2$ is also parallel to $\hat{\mathbf{n}}$. In practice this can be done by observing the reconstructed image of the surface through an objective with a small relative aperture (not shown in the figure).

At the second step, the flat-bottom probing hole is made using a rectangular-profile micro end mill, the hole axis being directed along axis Z (Fig. 2, *b*). After that, stresses σ_{ii}, τ_{ij} $(i, j \in x, y, z)$ existing in the material get

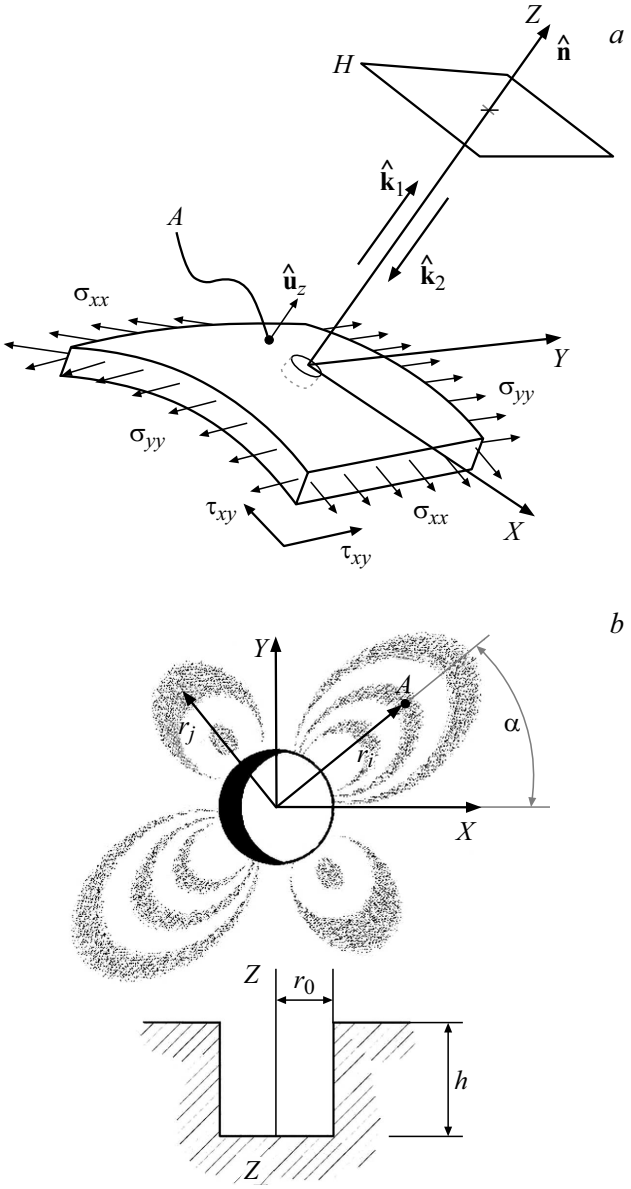

Figure 1. *a* — conditions for detecting normal displacements u_z in the probing hole vicinity by holographic interferometry; *b* — the probing hole geometry (the lower panel presents the profile). *A* is the surface point in the vicinity of the hole; u_z is the displacement component directed along axis *Z*; $\mathbf{k}_{1,2}$ are the wave vectors of the light illuminating point *A* and light scattered towards hologram *H* and observer, respectively; r_0 and *h* are the hole radius and depth, *r* is the radius-vector to the center of the *i*, *j*-th fringe. Angle α is specified for the condition when σ_1 act along r_i.

redistributed so as to compensate the absent bonds. The following surface displacements u_i will contain component u_z directed along axis *Z*. Since the desired relation is sought for only normal components of the displacement vector, then the smaller is the surface local curvature, the more accurate are the measurements.

At the third step, the wavefront reconstructed by the hologram and front scattered from the strained surface are observed simultaneously. Being coherent, both fronts interfere in the real-time mode. Sensitivity vector $\hat{\mathbf{K}} \equiv \hat{\mathbf{k}}_2 - \hat{\mathbf{k}}_1$ will be parallel to axis *Z* and, thus, the interferogram will be contributed exclusively by displacement component u_z. Since both $\hat{\mathbf{k}}_{1,2}$ vectors are collinear and equal in modulus ($K = 4\pi/\lambda$), the value of an interferometric fringe appears to be equal to half of wavelength λ of the used light. Indeed, interferential maxima or minima are related to wave phase difference $\delta = 2\pi N$, where $N = 0, 1, 2, \ldots$ is the fringe serial number (or, simply, the order). On the other hand, the phase difference is $\delta = Ku_z$; hence, assuming that $N = 1$ and equalizing these expressions, obtain the specified value $\Delta w_{N=1} = \lambda/2$. Notice that the axes of the fringe pattern symmetry are mutually orthogonal and coincide with the principal axes of stresses σ_1 and σ_2. This fact makes

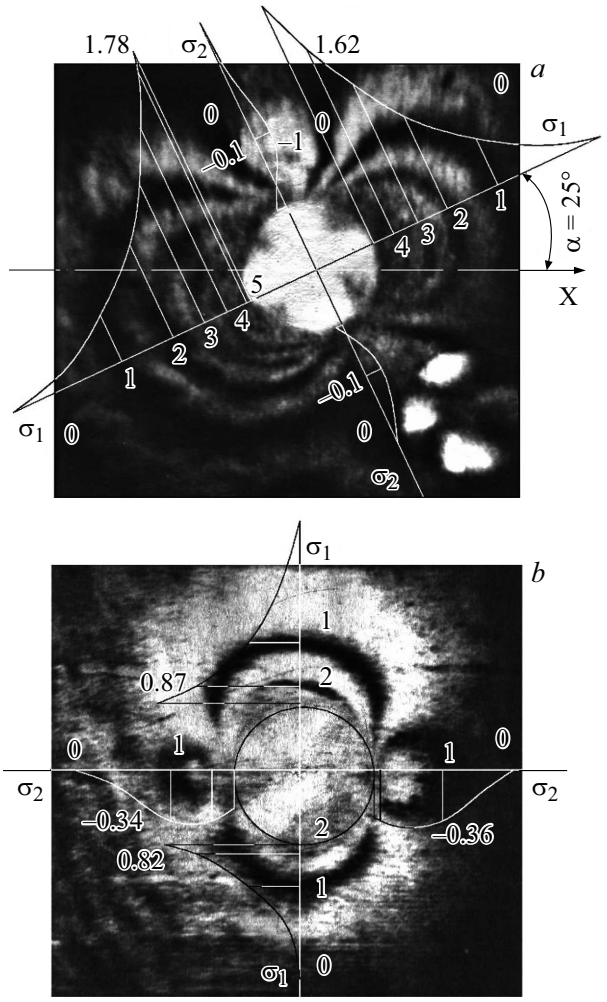

Figure 2. Case interferograms for duralumin sheet D16 40 mm thick which is free of residual strains. *a* — a probing hole with $r_0 = 1$ mm and $h = 2$ mm located on the end near-edge cross-section, $\sigma_1 \approx 49$ MPa, $\sigma_2 \approx -11$ MPa; *b* — a similar hole in the center of the cross-section with $\sigma_1 \approx -9$ MPa, $\sigma_2 \approx -17$ MPa. The figure axes, angle α in the laboratory frame of reference, and displacement epures approximated with formula (2) are shown. The digits correspond to orders *N* and displacement magnitudes (in μm).

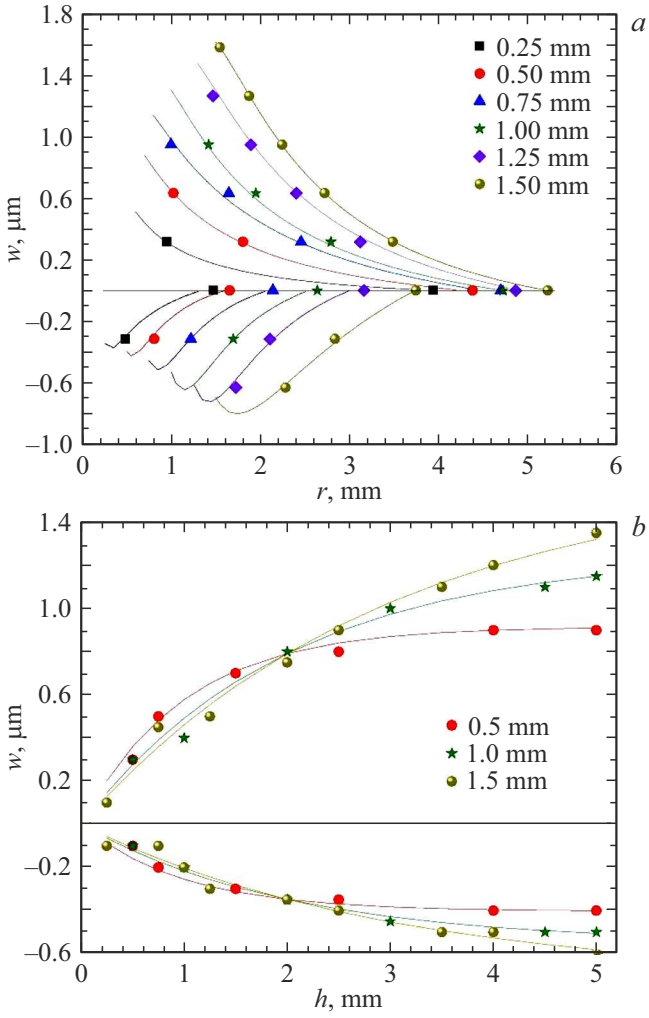

Figure 3. *a* — dependences of normal surface displacement w on distance r for different probing hole radii r_0 at fixed depth $h = 2r_0$; the dependences have been obtained for a test sample with $\sigma_1 = 240$ MPa, $\sigma_2 = -80$ MPa; *b* — displacement w at the hole edge ($r = r_0$) versus depth h at different r_0 for the same sample.

it possible to visualize the orientation of principal planes (Fig. 2).

The obtained interferogram contains information only on the absolute magnitudes of displacement but presents no data on the displacement direction or, in other words, sign. Let us assume it to be positive in the case of increasing path difference, i. e. of the surface displacement along $\hat{\mathbf{n}}$ inwards the body. The sign can be determined by displacing the hologram along axis Z. If the fringe order N at point A decreases, this means that directions of the hologram and surface displacements coincide, and vice versa. In practice, a quite insignificant test displacement is sufficient (about some tens of wavelength).

Based on the results of a series of experiments with test samples having probing holes 0.5 to 3.0 mm in diameter and 0.2 to 5.0 mm in depth, an empirical expression interrelating normal displacements and strains was obtained:

$$\varepsilon_3 = w\frac{2r_0}{r}h\left[1 - \exp\left(-\frac{h}{2r_0}\right)\right], \qquad (1)$$

where ε_3 is the strain along axis Z; r_0 and h are the hole radius and depth; r is the distance from the point on the sample surface and the drilling center measured along the interferogram symmetry axis (figure axis). In the case of constant stresses, an increase in radius r_0 leads to an increase in the surface displacement (Fig. 3, *a*); this, on the one hand, reduces the measurement error but, on the other hand, can give rise to plastic strains and thus distort the results. The exponential term was revealed in analyzing the interferograms obtained for holes of equal diameters but different depths (Fig. 3, *b*). In the course of the experiment, for each test sample there were performed series of interferometric measurements of displacements w, between which the hole depth w was successively increased. Number of fringes N changed significantly in the depth variation range $h = (0.5-5)r_0$; after $h = 5r_0$, variations in the order became lower than the drilling error (here $\Delta N = \pm 1/2$). The IFx46x dependence on r was assumed to be

$$w = \frac{A}{r^n} + \frac{B}{r^{n+2}} + C, \qquad (2)$$

, where A, B and C are the constants obtained by approximation. Then the stresses in the vicinity of the drilled hole may be found as via the Kirsch equations [6]. For instance, according to the Hookeś law,

$$-\frac{E\varepsilon_3^{(1)}}{\nu} = \sigma_1\left(1 - \frac{2r_0^2}{r^2}\right) - \sigma_2\left(1 + \frac{2r_0^2}{r^2}\right), \qquad (3)$$

where ν is the Poisson ratio, $\varepsilon_3^{(1)}$ is the relative strain in the σ_1 direction. Strain component $\varepsilon_3^{(2)}$ in the orthogonal direction may be expressed in the similar way:

$$-\frac{E\varepsilon_3^{(2)}}{\nu} = \sigma_2\left(1 - \frac{2r_0^2}{r^2}\right) - \sigma_1\left(1 + \frac{2r_0^2}{r^2}\right). \qquad (4)$$

The final expression for principal stresses, which was obtained by jointly solving equations (3) and (4), has the following form:

$$\sigma_{1,2} = -E\frac{\pm\varepsilon_i r_i^2(r_j^2 \pm 2r_0^2) \mp \varepsilon_j r_j^2(r_i^2 \pm 2r_0^2)}{4\nu r_0^2(r_i^2 - r_j^2)}, \qquad (5)$$

where $r_{i,j}$ is the coordinate of the i, j-th fringe center measured along the figure axes (Fig. 1, *b*), while $\varepsilon_{i,j}$ is the relative strain corresponding to it. Using (5), it is possible to reduce the effect of plastic strains arising at the hole edge in the process of its fabrication on the stress magnitudes to be determined. In interpreting the interferograms obtained on the test samples, stresses differed from theoretical ones by no more than $(2-3)\cdot 10^{-4}E$, where E is the Youngś modulus of the material.

In conclusion, let us mention briefly the restrictions imposed by the proposed method on the object under study. First, stress component σ_3 directed along the hole axis is assumed to be absent. Second, according to the Saint-Venant principle, the distance between the center of the hole and its edge or any other violation of the object continuity should be not shorter than $5r_0$. Third, the surface curvature should not be significant, and the probing hole axis should be directed normally to the surface. The illumination and observation directions should be made parallel to the hole axis in order to minimize the contribution of tangential displacements.

Conflict of interests

The authors declare that they have no conflict of interests.

References

[1] A.A. Antonov, A.I. Bobrik, V.K. Morozov, G.N. Chernyshev, Izv. AN SSSR. Mekhanika tverdogo tela, № 2, 182 (1980). (in Russian)
[2] L.M. Lobanov, B.S. Kasatkin, V.V. Pivtorak, S.G. Andrushchenko, DAN SSSR, **271** (3), 557 (1983). (in Russian)
[3] G.N. Chernyshev, A.L. Popov, V.M. Kozintsev, I.I. Ponomarev, *Ostatochnye napryazheniya v deformiruemykh tverdykh telakh* (Fizmatlit, M., 1996). (in Russian)
[4] K. Duan, C.Y. Kwok, J. Geophys. Res. Solid Earth, **121**, 2361 (2016). DOI: 10.1002/2015JB012676
[5] Y. Wang, X. Zhong, S. Nie, Y. Zhu, C. Chen, Processes, **11**, 1150 (2023). DOI: 10.3390/pr11041150
[6] G. Kirsch, Zantralblatt Verlin Deutscher Ingenieure, **42**, 797 (1898).

Translated by Solonitsyna Anna